Glycosylation of acyl carrier protein-bound polyketides during pactamycin biosynthesis

Auday A. Eida[1], **Mostafa E. Abugrain**[1], **Corey J. Brumsted**[2], **Taifo Mahmud**[1,2]

[1]Department of Pharmaceutical Sciences, Oregon State University, Corvallis, Oregon 97331-3507, USA;

[2]Department of Chemistry, Oregon State University, Corvallis, Oregon 97331-4003, USA

Abstract

Glycosylation is a common modification reaction in natural products biosynthesis and has been known to be a post assembly line tailoring process in glycosylated polyketide biosynthesis. Here, we show that in pactamycin biosynthesis glycosylation can take place on an acyl carrier protein (ACP)-bound polyketide intermediate. Using *in vivo* gene inactivation, chemical complementation, and *in vitro* pathway reconstitution we demonstrate that the 3-aminoacetophenone moiety of pactamycin is derived from 3-aminobenzoic acid by a set of discrete polyketide synthase proteins via a 3-[3-aminophenyl]3-oxopropionyl-ACP intermediate. This ACP-bound intermediate is then glycosylated by an *N*-glycosyltransferase, PtmJ, providing a sugar precursor for the formation of the aminocyclopentitol core structure of pactamycin. This is the first example of glycosylation of a small molecule while tethered to a carrier protein. Additionally, we demonstrate that PtmO is a hydrolase that is responsible for the release of the ACP-bound product to a free β-ketoacid that subsequently undergoes decarboxylation.

Glycosylation is one of the most ubiquitous and important transformations in nature and plays a central role in the structural and physiological aspects of living organisms. Glycosyltransferases are the family of enzymes that catalyze glycosylation, resulting in sugar-containing products. In natural products biosynthesis, glycosylation is generally considered to be a tailoring process that takes place later in the pathway after the backbone structure is formed. Some exceptions apply to certain natural products when glycosylation is directly involved in the formation of the core structure. Such phenomenon has been proposed to occur in the biosynthesis of at least two highly important microbial natural products, mitomycin and pactamycin.[1–3]

Pactamycin (**1**) is a potent antitumor antibiotic produced by *Streptomyces pactum* ATCC 27456 with a unique chemical structure having a highly decorated aminocyclopentitol core unit, a 3-aminoacetophenone (3AAP, **2**), a 6-methylsalicylic acid (6MSA), and a *N,N*-dimethylurea (Figure 1a). It has been proposed that the core cyclopentitol unit is derived from glucose (Glc) or *N*-acetylglucosamine (GlcNAc), presumably through an unprecedented rearrangement mechanism.[4] The 3AAP moiety is derived from 3-aminobenzoic acid (3ABA, **3**), a product of dehydroshikimic acid (DHS) catalyzed by a unique PLP-dependent aminotransferase-aromatase enzyme, PtmT (Figure 1b), which is called PctV in another pactamycin cluster in *S. pactum* NBRC 13433 (Supplementary Table 1).[5–8] The 6MSA moiety is produced by the iterative type I polyketide synthase PtmQ.[3] A number of tailoring processes, *e.g.*, amination, carbamoylation (urea formation), *C*- and *N*-methylations, and hydroxylation, are involved in the pathway and result in a highly decorated aminocyclopentitol unit that is rich in stereocenters.[9,10]

Although direct involvement of 3ABA in pactamycin has been established,[5,6] the process underlying its conversion to the 3AAP moiety is not well understood. On the basis of the putative functions of genes within the pactamycin cluster (Figure 1c), two plausible pathways to the 3AAP moiety have been proposed. The first one involves a putative AMP-forming acyl-CoA synthetase, PtmS, which may convert 3ABA to 3ABA-AMP, followed by coupling between 3ABA-AMP and acetyl-CoA to give β-ketoacyl CoA ester.[2] Hydrolysis of the β-ketoacyl-CoA by a putative hydrolase/acyltransferase (PtmO) followed by a decarboxylation reaction would give 3AAP (Figure 1b, path I).[2]

The other pathway involves PtmS and discrete polyketide enzymes, PtmI (an acyl carrier protein, ACP), PtmK (a β-ketoacyl-ACP synthase, KAS), and a putative hydrolase/acyltransferase, PtmO (Figure 1b, path II).[3] PtmK is similar to KAS I/II, which is responsible for the elongation steps in fatty acid biosynthesis.[11,12] In this scenario, PtmS is proposed to activate 3ABA and load it to the ACP PtmI, whereas PtmK is proposed to catalyze condensation between 3ABA-ACP and malonyl-ACP. The product is then cleaved from the ACP (PtmI) by the putative hydrolase/acyltransferase PtmO. However, no experimental evidence is available to support either of the above pathways.

The mode of formation of the cyclopentitol unit in pactamycin is also unknown. Through incorporation studies using isotopically labeled precursors, Rinehart and co-workers showed that this portion of the molecule is derived from glucose, and more likely via *N*-acetylglucosamine (GlcNAc).[4] Available genetic information suggests that a radical SAM-dependent enzyme (PtmC), a putative glycosyltransferase (PtmJ), and a putative deacetylase (PtmG) may be involved in the formation of the cyclopentitol core, and this process may be similar to the formation of the mitosane core structure during mitomycin biosynthesis.[1–3] In mitomycin biosynthesis, however, D-glucosamine (or its derivative) is assembled into the mitosane unit through condensation with 3-amino-5-hydroxybenzoic acid (AHBA). Although details for this reaction are not available, it was proposed that MitB, a protein with similarity to PtmJ, mediates the condensation reaction, followed by an unknown mechanism to complete the C-C bond formation.[13] In fact, the glycosyltransferase PtmJ from *S. pactum* has been shown to catalyze a coupling reaction between UDP-*N*-acetyl-α-D-glucosamine and 3AAP.[2] The product would then need to undergo deacetylation, possibly by the *N*-

deacetylase homologue PtmG followed by a radical-mediated rearrangement by PtmC to form the cyclopentitol ring structure. Inactivation of the *ptmC* and *ptmJ* genes indeed abolished the production of pactamycin, demonstrating their importance in the early biosynthetic steps.[3]

Despite the ability of PtmJ to glycosylate 3AAP *in vitro*, our incorporation studies showed that 3AAP is not able to rescue the production of pactamycin in the *ptmT* mutant strain of *S. pactum*, which lacks the ability to produce 3ABA,[5] suggesting that 3AAP is not a free intermediate in the pactamycin pathway. Consequently, the mode of formation of the 3AAP unit in pactamycin biosynthesis and the timing of the glycosylation reaction catalyzed by PtmJ remained unclear. Here, we employed *in vivo* gene inactivation, chemical complementation, and *in vitro* pathway reconstitution using six purified recombinant proteins to interrogate the formation of the 3AAP unit of pactamycin and the timing of the glycosylation reaction. The results not only provided new insights into the biosynthesis of pactamycin, but also revealed an interesting and unprecedented phenomenon where glycosylation occurs on a polyketide intermediate while it is still attached to a carrier protein.

RESULTS

Involvement of discrete polyketide synthase proteins.

To explore the role of *ptmI*, *ptmK*, and *ptmO* in pactamycin biosynthesis, these genes were inactivated in *ptmH* mutant strain that produces pactamycin analogues,[14] TM-025 (**4**) and TM-026 (**5**) (Supplementary Figures 1 and 2). The *ptmH* mutant was used because TM-025 and TM-026 are chemically more stable and produced in higher yields than pactamycin. ESI-MS analysis of the products revealed that inactivation of *ptmI*, *ptmK*, or *ptmO* in the *ptmH* strain entirely abolished the production of TM-025 and TM-026 (Supplementary Figure 3). In addition, the mutants did not give any detectable intermediates, indicating that the gene products are involved early in the pathway.[3,14] Chemical incorporation experiments with 3ABA in these mutants also did not give any products, consistent with the notion that these discrete polyketide synthase enzymes play a role in the conversion of 3ABA to the 3AAP moiety.

Evaluation of *N*-acetylcysteamine thioesters.

Based on the above results, we hypothesized that 3ABA is activated by PtmS and loaded onto the acyl carrier protein PtmI. Claisen condensation between 3ABA-ACP and malonyl-ACP catalyzed by PtmK would give 3-[3-aminophenyl]3-oxopropionyl-ACP (3AP-3OP-ACP). To test this hypothesis, *N*-acetylcysteamine (NAC) thioesters of 3ABA and 3-[3-aminophenyl]3-oxopropionate (3AP-3OP), which mimics the β-ketoacyl-ACP, were synthesized (Supplementary Note 1) and added to the cultures of the 3ABA-lacking *ptmH*/ *ptmT* mutant.[5] ESI-MS and MS/MS analyses of the culture broths of the *ptmH*/ *ptmT* mutant fed with 3ABA-SNAC or 3AP-3OP-SNAC revealed the recovery of TM-025/ TM-026 production by the mutant (Figures 2a–2f, and Supplementary Figure 4), providing strong evidence for the involvement of 3ABA-ACP and 3AP-3OP-ACP in pactamycin biosynthesis.

Isolation of GlcNAc-3AAP from complemented mutants.

While 3AP-3OP-SNAC was able to complement the lack of 3ABA in *ptmH*/ *ptmT* and rescued the production of TM-025 and TM-026 in the mutant, it was not able to recover the production of pactamycin or TM-025/TM-026 when added to the cultures of *ptmS*,[10] *ptmI*,[10] *ptmK*::*aac(3)IV*,[10] *ptmH*/ *ptmI*, and *ptmH*/*ptmK*::*aac(3)IV* mutants (Supplementary Figures 5 and 6). The *ptmK*::*aac(3)IV* mutant is *S. pactum* in which the *ptmK* gene has been disrupted by a plasmid harboring the apramycin resistant gene *aac(3)IV*. This suggests that the discrete PKS proteins may work in concert and that the synthetic β-ketoacyl intermediate has to be initially loaded onto PtmI, presumably through the ketosynthase PtmK (Figure 2g). Interestingly, instead of recovering the production of pactamycin or TM-025/TM-026, the addition of 3AP-3OP-SNAC to these mutants led to another product with a molecular formula of $C_{16}H_{22}N_2O_6$ (*m/z* 361.1370 $[M+Na]^+$) (Supplementary Figures 5 and 6). Direct comparisons of this product with synthetically prepared authentic compound (Supplementary Note 2) confirmed the identity of the product to be GlcNAc-3AAP (**6**). This product may be formed from unspecific hydrolysis of the NAC thioester, and the resulting β-ketoacid undergoes non-enzymatic decarboxylation to give 3AAP, which is subsequently glycosylated by the glycosyltransferase PtmJ to give GlcNAc-3AAP (Figure 2g). The accumulation of GlcNAc-3AAP in the culture suggests that it is not an intermediate in pactamycin biosynthesis as previously suggested.[2] This was further confirmed by adding GlcNAc-3AAP to cultures of *ptmH*/ *ptmT* and *ptmJ* mutants, in which no recovery of pactamycin production was observed. Similarly, incorporation experiments with 3AAP in cultures of *ptmH*/ *ptmT* and *ptmJ* mutants also did not give any pactamycin products, confirming 3AAP and GlcNAc-3AAPare not involved in the pactamycin pathway.

To determine if glycosylation occurs prior to the PKS reaction (i.e., on 3ABA), GlcNAc-3ABA was synthesized (Supplementary Note 3) and added to cultures of *ptmH*/ *ptmT* and *ptmJ* mutants. MS analysis of the culture broths showed the recovery of pactamycin analogue production in the *ptmH*/ *ptmT* mutant, but paradoxically no pactamycin production was observed in the *ptmJ* mutant (Supplementary Figure 7). As GlcNAc-3ABA was not able to salvage the production of pactamycin without the presence of the glycosyltransferase PtmJ, it may be assumed that the compound was not incorporated into the pathway intact. Indeed, doubly isotope-labeled [^{13}C]GlcNAc-[^{13}C]3ABA, which was synthesized (Supplementary Note 4) and added to the cultures of the 3ABA-lacking *ptmH*/ *ptmT* mutant, gave isotopically labeled products (TM-025 and TM-026) that only bear a single isotope (^{13}C atom) with the *m/z* values of 396.19 and 530.23, respectively (Supplementary Figure 8). Therefore, it may be concluded that [^{13}C]GlcNAc-[^{13}C]3ABA had undergone hydrolysis to [^{13}C]3ABA, which was then incorporated into the pathway to produce [^{13}C]TM-025 and [^{13}C]TM-026 (Supplementary Figure 8). This isotope experiment not only explains why GlcNAc-3ABA was not able to rescue the production of pactamycin in the *ptmJ* mutant, but also excludes the possibility that glycosylation occurs prior to the polyketide formation.

In vitro characterization of PtmS.

To demonstrate explicitly the involvement of the discrete polyketide synthase proteins PtmS, PtmI, PtmK, and PtmO in the formation of the 3AAP moiety, the genes were cloned, and the products were characterized *in vitro*. The putative AMP-forming acyl-CoA synthetase PtmS was predicted to catalyze the activation of the starter unit 3ABA to its AMP derivative. Therefore, the gene was cloned into a pMBP28b vector and expressed in *E. coli* BL21(DE3)pLysS to obtain soluble His6-tagged maltose binding protein-fused PtmS (Supplementary Figure 9). Subsequently, the purified protein was incubated with 3ABA in the presence of ATP and $MgCl_2$ to give 3-aminobenzoyl-AMP (3ABA-AMP), which was validated by HPLC and LC-MS (Supplementary Figure 10), confirming the function of PtmS as an AMP-ligase (Figure 3a). The relative yield of 3ABA-AMP, estimated from the amount of inorganic diphosphate produced in the reaction,[15,16] was ~63% (Supplementary Figure 11).

PtmI serves as a carrier for 3ABA and malonyl unit.

As *ptmI* is the only gene encoding a discrete acyl-carrier protein (ACP) within the pactamycin biosynthetic gene cluster, we propose that PtmI would act as a carrier protein for both the 3ABA starter unit and the malonyl extender unit. A putative 4´-phosphopantetheinyl transferase (PPTase) gene, *ptmP*, was also found in the cluster, suggesting its role in converting the inactive apo-PtmI to the active holo-PtmI. PtmP may also be responsible for the activation of the ACP domain of PtmQ. The latter protein shares high similarity with the iterative type I PKS, ChlB1, which is involved in the biosynthesis of 6-methylsalicylic acid (6MSA) in *S. antibioticus*.[17] Gene inactivation and heterologous expression experiments have confirmed the activity of PtmQ as a 6MSA synthase.[3]

To determine the function of PtmI, the gene was cloned in pACYCDuet-1, independently and together with the putative PPTase gene *ptmP*, and expressed in *E. coli* BL21(DE3)pLysS. While the expression of *ptmI* could be induced by IPTG to give soluble recombinant PtmI (Figures 3b and Supplementary Figure 12), no clear expression of *ptmP* was observed. Subsequently, the broad spectrum PPTase gene *sfp* from *Bacillus subtilis* was cloned in pET28a expression vector and soluble recombinant Sfp was obtained (Supplementary Figure 9). The construct was then introduced into *E. coli* BL21(DE3)pLysS that harbors pACYCDuet-1/*ptmI* to give soluble Sfp and holo-PtmI (12,393.50 Da) as confirmed by HPLC (Supplementary Figure 12) and LC-MS (Figure 3c). Posttranslational gluconoylation (Gluc) of the holo-PtmI was also observed (12,571.50 Da). The holo-PtmI and its Gluc analogue were then incubated with PtmS and 3ABA for 7 h to give 3ABA-PtmI (12,513.20 Da) and its Gluc analogue (12,691.20 Da) (relative yield ~98%, as estimated from the amount of AMP produced in the reaction)[18] (Figure 3d and Supplementary Figure 13).

Incubation of the holo-PtmI with malonyl-CoA (Figure 3a) also led to the formation of malonyl-PtmI (12,479.90 Da) and its Gluc analogue (12,658.00 Da) (Figure 3e), confirming the role of PtmI as a carrier protein for both 3ABA and malonyl moieties. This set the stage for a subsequent coupling reaction between the 3ABA starter unit and the malonyl extender unit by a putative β-ketoacyl-ACP synthase, PtmK.

Characterization of the β-ketoacyl-ACP synthase PtmK.

PtmK is similar to β-ketoacyl-ACP synthase (KAS) I and II, which are responsible for the elongation steps in fatty acid biosynthesis.[11,12] Since isotope incorporation experiments have shown that the methyl group present in the 3AAP unit is derived from C-2 of acetate, PtmK has been predicted to be involved in this extension. To characterize the function of PtmK, the gene was cloned into pET28a and expressed in a tunable T7 expression strain, *E. coli* Lemo21(DE3), to provide soluble His$_6$-tagged PtmK, which is then purified by a Nickel-NTA column (Supplementary Figure 9). Incubation of PtmK with 3ABA-PtmI for 12 h, followed by incubation with malonyl-PtmI for 16 h yielded a mass consistent with 3-[3-aminophenyl]3-oxopropionyl-PtmI (12555.20 Da) (Figure 3f), demonstrating the involvement of discrete polyketide synthase proteins in the formation of 3-aminoacetophenone (3AAP) moiety of pactamycin. It is worth noting that acetyl-PtmI (12436.60 Da), a decarboxylation product of malonyl-PtmI, was significantly produced in the reaction mixture (Figure 3f), indicating a high tendency of protonation of the decarboxylated intermediate. This was only conspicuously observed when PtmK was present and further validates the decarboxylative activity of PtmK.

PtmO is responsible for premature release of 3AP-3OP.

The formation of GlcNAc-3AAP from 3AP-3OP-SNAC in the cultures of *ptmS*, *ptmI*, *ptmK*, *ptmH*/*ptmI*, and *ptmH*/*ptmK::aac(3)IV* mutants may be due to unspecific hydrolysis of the NAC thioester by the putative hydrolase PtmO, followed by non-enzymatic decarboxylation. The product is then glycosylated by PtmJ to generate the shunt metabolite GlcNAc-3AAP. To confirm this, 3AP-3OP-SNAC was added to a culture of the *ptmO* mutant. As expected, the mutant neither produced pactamycin nor GlcNAc-3AAP (Supplementary Figure 14), supporting the hydrolytic function of PtmO and its role in pactamycin biosynthesis. This was subsequently confirmed by incubating 3AP-3OP-PtmI with purified recombinant PtmO, which gave 3AAP as a product (Figure 4). No product was observed when boiled PtmO was used (Figure 4b), which unambiguously established that PtmO is a hydrolase, and that the β-ketoacid product can undergo a spontaneous decarboxylation reaction. This is consistent with our observation that synthetically prepared 3AP-3OP can convert to 3AAP without an enzyme. However, as 3AAP and its glycosylated product are not involved in pactamycin biosynthesis, the timing of this hydrolysis remains unclear, but it should occur later in the pathway after further modification(s) of 3AP-3OP-PtmI.

PtmJ is a promiscuous glycosyltransferase.

Although GlcNAc-3AAP is not an intermediate in the pactamycin pathway, its production by the *S. pactum* strains when incubated with 3AAP indicates the relaxed substrate specificity of PtmJ. In addition to 3AAP, PtmJ can also glycosylate phenylamines such as aniline (AN), 3-fluoroaniline (3FAN), and 4-fluoroaniline (4FAN). Addition of these compounds to the cultures of *ptmH*/*ptmT* mutant resulted in the production of GlcNAc-AN, GlcNAc-3FAN, and GlcNAc-4FAN (Supplementary Figures 15 and 16). Some of the products were isolated chromatographically and their chemical structures were characterized by NMR (Supplementary Figures 17 and 18). Interestingly, besides the GlcNAc products,

glucosyl aniline (Glc-AN), Glc-3FAN, and Glc-4FAN (Supplementary Figures 15 and 16) were also produced, suggesting that PtmJ not only recognizes NDP-GlcNAc, but also NDP-glucose, as donor sugar. Addition of 3AAP and 4FAN individually to cultures of the *ptmJ* mutant[3] did not give any glycosylated 3AAP or 4FAN (Supplementary Figures 19 and 20), ruling out the possibility that other glycosyltransferases are involved in the reaction and confirming that PtmJ is the sole enzyme responsible for the formation of the glycosylated arylamines. Interestingly, despite its structure similarity to 3AAP, 3ABA was not processed by PtmJ (Supplementary Figure 21).

The timing of glycosylation in pactamycin biosynthesis.

As neither 3ABA nor 3AAP is the natural substrate for PtmJ, the glycosylation reaction is predicted to take place during the conversion of 3ABA to the 3AAP moiety, which involves the discrete polyketide synthase enzymes PtmS, PtmI, and PtmK (Figure 3). Therefore, it may be proposed that the substrate for PtmJ is an ACP-bound polyketide intermediate. To determine if PtmJ is able to catalyze the glycosylation of 3ABA-ACP and/or 3AP-3OP-ACP *in vitro*, the gene was cloned in pET28a and expressed in *E. coli* Lemo21(DE3) to give soluble His$_6$-tagged PtmJ. The purified protein was subsequently incubated with 3ABA-ACP or 3AP-3OP-ACP for 10 h in the presence of UDP-GlcNAc. 3ABA-ACP was generated in a one-pot reaction containing 3ABA, PtmS, PtmI/Sfp, ATP, and MgCl$_2$ for 7 h (Figure 5a), whereas 3AP-3OP-ACP was generated from the same one-pot reaction condition but with subsequent incubation with PtmK for 12 h followed by incubation with malonyl-ACP for 16 h. LC-MS analysis of the reaction mixtures containing PtmJ revealed the formation of GlcNAc-3ABA-ACP (12716.20 Da) (Figure 5b) and GlcNAc-3AP-3OP-ACP (12758.40 Da) (Figure 5c), validating the notion that glycosylation can occur on an ACP-bound polyketide intermediate in pactamycin biosynthesis. Further experiments using deuterated 3ABA (3ABA-2,4,5,6-d_4) as substrate provided GlcNAc-3ABA-d_4-PtmI (12720.40 Da) and GlcNAc-3AP-3OP-d_4-PtmI (12762.40 Da) (Figure 5d), which unambiguously demonstrated the formation of glycosylated 3ABA-ACP and 3AP-3OP-ACP. Reaction mixtures containing boiled PtmJ did not produce any glycosylated products (Figure 5e), confirming the role of PtmJ in the glycosylation reactions. This is the first direct evidence for the glycosylation of an ACP-bound polyketide intermediate in natural product biosynthesis. The relative yield of GlcNAc-3ABA-PtmI, as estimated from the amount of UDP produced in the reaction measured by the coupled colorimetry assay using pyruvate kinase and lactate dehydrogenase,[19] was ~58% (Supplementary Figure 22). On the other hand, the average yield of GlcNAc-3AP-3OP-ACP, as estimated from the mass spectral data, was about 36% (Supplementary Table 2).

PtmK functions as a gatekeeper.

Although PtmJ can glycosylate both 3ABA-ACP and 3AP-3OP-ACP *in vitro*, it may be contemplated that only one of these compounds is the preferred natural substrate for the enzyme. Moreover, our study above has shown that the ketosynthase PtmK can catalyze a Claisen condensation between 3ABA-ACP and malonyl-ACP to give 3AP-3OP-ACP, but it was not clear if PtmK can process glycosylated 3ABA-ACP (GlcNAc-3ABA-ACP) to give GlcNAc-3AP-3OP-ACP. Accordingly, a set of experiments was designed to investigate the substrate specificity of PtmK and evaluate if GlcNAc-3ABA-PtmI can be processed by the

enzyme. While GlcNAc-3ABA-PtmI may be produced from 3ABA-PtmI using PtmJ and UDP-GlcNAc, the product needed to be separated from the unreacted 3ABA-PtmI, PtmJ or UDP-GlcNAc before subjecting it to the subsequent reactions, as the presence of the remaining 3ABA-PtmI in the mixture may be processed by PtmK and subsequently by PtmJ to give GlcNAc-3AP-3OP-PtmI. However, attempts to separate GlcNAc-3ABA-PtmI from PtmJ or UDP-GlcNAc using size-exclusion filters were not successful. Therefore, 3ABA-SNAC, which resembles 3ABA-ACP, was used to produce GlcNAc-3ABA-SNAC, which was then separated, together with the remaining 3ABA-SNAC, from MeOH-denatured PtmJ (Figures 6a and 6b). Incubation of 3ABA-SNAC and GlcNAc-3ABA-SNAC with PtmK for 12 h followed by 16 h incubation with malonyl-PtmI only gave 3AP-3OP-PtmI (β-ketoacyl-ACP) (Figure 6c), revealing that only 3ABA-SNAC was processed by PtmK, whereas GlcNAc-3ABA-SNAC was not. Therefore, while 3ABA-PtmI can be glycosylated by PtmJ *in vitro*, the product cannot be processed by the ketosynthase PtmK, suggesting that only glycosylation of the ACP-bound β-keto intermediate 3AP-3OP-PtmI is relevant to pactamycin biosynthesis.

DISCUSSION

3-Aminobenzoic acid (3ABA) is a small molecule commonly used in synthetic organic chemistry, but its occurrence in nature is extremely rare.[5,6] In pactamycin biosynthesis, 3ABA has been shown to be the precursor of the 3AAP moiety, but details of the transformation including enzymes that are involved in the transformation were elusive.[4,5,20] In this study, we show that the conversion of 3ABA to the 3AAP moiety is catalyzed by a set of discrete polyketide synthase enzymes, PtmS, PtmI, PtmK, and PtmO. PtmS is an adenylate forming enzyme,[21] which converts 3ABA to 3ABA-AMP; the product is then loaded to the ACP PtmI. It shares moderate sequence similarity to the adenylation domains in the loading modules of the rifamycin and ansamitocin PKSs (31.5 % identity with the RifA adenylation domain and 31.1 % identity with the AsmA adenylation domain).[22,23] These domains are part of multifunctional multimodular type I polyketide synthases that convert 3-amino-5-hydroxybenzoic acid (AHBA) to AHBA-AMP, which is then loaded onto the acyl carrier protein (ACP) domains of the enzymes.[23,24] PtmK is similar to β-ketoacyl-ACP synthases (KAS) I/II, which are responsible for the elongation steps in fatty acid biosynthesis.[11,12] Another stand-alone KAS protein (PtmR) in the pathway was also considered as a candidate enzyme involved in 3AAP formation; however, an earlier study revealed that this protein is involved in the tailoring process of pactamycin.[10] While PtmS, PtmI, and PtmK are discrete polyketide synthase proteins, they also appear to function more effectively when working in concert, which is consistent with some other discrete polyketide synthase proteins.[25,26] The ability of 3AP-3OP-SNAC to rescue the production of TM-026 in Δ*ptmH*/Δ*ptmT* but not in mutant strains lacking either one of the PKS genes supports this notion. However, our study also shows that the loading of malonyl to PtmI can take place by its intrinsic self-acylation property. Further detailed studies are necessary to illuminate the nature of interactions between these discrete polyketide proteins.

Although 3AAP and GlcNAc-3AAP have been proposed to be part of pactamycin biosynthesis,[2] these compounds appeared to have no direct involvement in the pathway. Incorporation experiments and biochemical studies have also ruled out the possibility of

glycosylation of 3ABA. On the other hand, 3ABA-SNAC and 3AP-3OP-SNAC, which resemble acyl carrier protein-bound substrates, were both able to rescue the production of TM-025/TM-026 in *ptmH/ ptmT*, indicating the role of PKS in 3AAP formation. While it is possible that 3ABA-SNAC is hydrolyzed to 3ABA prior to incorporation into the pathway, hydrolysis of 3AP-3OP-SNAC and spontaneous decarboxylation will result in 3AAP, which is not involved in pactamycin biosynthesis. Therefore, the production of TM-026 by *ptmH/ ptmT* when incubated with 3AP-3OP-SNAC strongly suggests that 3AP-3OP-ACP is indeed involved in the pathway and the glycosylation reaction should take place on an ACP-bound polyketide intermediate.

The above results were validated by reconstituted enzymatic assays using purified recombinant PtmS, PtmI, PtmK, PtmJ, and PtmO. The formation of 3AP-3OP-PtmI from a concerted catalytic function of PtmS, PtmI, and PtmK strongly suggests that 3AP-3OP-PtmI is involved in the pactamycin pathway. The PtmI-bound intermediate is then glycosylated by the glycosyltransferase PtmJ. This is an unusual phenomenon that hitherto has never been reported. Although in the *in vitro* assay PtmJ can also glycosylate 3ABA-PtmI, the glycosylated product is not processed by the subsequent enzyme, the ketosynthase PtmK. Thus, PtmK appears to function as a gatekeeper that only selects 3ABA-PtmI for the Claisen condensation. This result strongly suggests that in pactamycin biosynthesis glycosylation takes place after the formation of 3AP-3OP-PtmI. While there is no evidence to negate the possibility that the glycosylation of 3ABA-PtmI may also occur *in vivo*, one would expect that such unproductive biotransformation would be regulated by negative feedback and/or equilibrium between biosynthetic intermediates.[27]

Furthermore, the fact that GlcNAc-3AAP is not directly involved in pactamycin biosynthesis also suggests that additional modifications of the sugar moiety are required before the glycosylated β-ketoacyl product is cleaved from the ACP. These modifications may involve the oxidoreductase PtmN, the aminotransferase PtmA, the carbamoyltransferase PtmB, the deacetylase PtmG, the radical SAM-dependent C-methyltransferases PtmL and PtmM, and/or rearrangement and cyclization to an aminocyclopentitol intermediate by the radical SAM protein PtmC.[2,3,28]

PtmJ is a putative GT-A type protein belonging to family 2 of the glycosyltransferase superfamily. Members of this family include chitin synthases, *N*-acetylglucosaminyltransferases, and hyaluronan synthases.[29] However, BLAST analysis indicated that there were only a few proteins reported in the NCBI database that are similar to PtmJ. The most similar ones are putative glycosyltransferases from *Streptomyces* sp. (WP_079057159.1, 71.20 % identity), *Streptomyces acidiscabies* (WP_078841237.1, 72.76 % identity), and *Streptomyces griseoruber* (WP_099054043.1, 68.71 % identity), which also seem to be part of the pactamycin clusters in those organisms. More interestingly, PtmJ is highly promiscuous with the ability to not only glycosylate small molecules but also protein-bound substrates. In fact, many enzymes in the pactamycin pathway have broad substrate specificity. Those include the *N*-methyltransferase PtmD, the acyltransferase PtmR, and the 7-hydroxylase, for which the gene is still unknown.[9,10] However, the ability of PtmJ to catalyze the glycosylation of a polyketide intermediate while it is still attached to an ACP is unprecedented.

In conclusion, this study reveals new insights into the formation of 3AAP moiety of pactamycin, involving a set of discrete polyketide synthase proteins, and demonstrates the glycosylation of an ACP-bound polyketide intermediate by a highly broad-spectrum glycosyltransferase, PtmJ. In addition, we validated that PtmO is a hydrolase enzyme that is responsible for the release of the glycosylated β-ketoacid product from the ACP, and the free β-ketoacid subsequently undergoes decarboxylation.

METHODS

General.

All chemicals were obtained either from Sigma Aldrich, EMD, TCI, or Pharmacia. All reactions were carried out under an inert, Argon atmosphere in oven-dried glassware at 170°C unless indicated otherwise. Benzene (PhH), Methylene chloride (CH_2Cl_2), and triethylamine (Et_3N) were distilled over calcium hydride prior to use. All other reagents and solvents were used without further purification from commercial sources. Analytical thin-layer chromatography (TLC) was performed using silica gel plates (60 Å), which were visualized using a UV lamp, ceric ammonium molybdate (CAM), potassium permanganate, iodine, or vanillin stains. Chromatographic purification of products was performed on silica gel (60 Å, 72–230 mesh). Proton NMR spectra were recorded on Bruker 400, 500, or 700 MHz spectrometers. Proton chemical shifts are reported in ppm (δ) relative to the residual solvent signals as the internal standard. Multiplicities in the ^{1}H NMR spectra are described as follows: s = singlet, bs = broad singlet, d = doublet, bd = broad doublet, t = triplet, bt = broad triplet, q = quartet, m = multiplet; coupling constants are reported in Hz. Carbon NMR spectra were recorded on Bruker 500 or 700 MHz spectrometers. Carbon chemical shifts are reported in ppm (δ) relative to the residual solvent signals as the internal standard. Low-resolution electrospray ionization (ESI) mass spectra were recorded on a Thermo-Finnigan liquid chromatograph-ion trap mass spectrometer. High-resolution ESI mass spectra were recorded on a ThermoElectron LTQ-Orbitrap Discovery mass spectrometer with a dedicated Accela HPLC system. FT-IR spectra were obtained on NaCl plates with a PerkinElmer Spectrum Vision spectrometer.

General DNA manipulations.

Genomic DNA of *S. pactum* ATCC 27456 was prepared by standard protocol[30] or using the DNeasy Tissue Kit (QIAGEN). DNA fragments were recovered from an agarose gel by using the QIAquick Gel Extraction Kit (QIAGEN). Restriction endonucleases were purchased from Invitrogen or Promega. Preparation of plasmid DNA was done by using a QIAprep Spin Miniprep Kit (Promega). All other DNA manipulations were performed according to standard protocols.[30,31] PCR was performed in 30 cycles by using a Mastercycler gradient thermocycler (Eppendorf) and Platinum *Taq* high fidelity DNA polymerase (Invitrogen). Oligodeoxyribonucleotides for PCR primers were synthesized by Sigma-Genosys. The nucleotide sequences of the gene fragments were determined at the Center for Genome Research and Biocomputing (CGRB) Core Laboratories, Oregon State University. ORFs were analyzed by FramePlot[32] analysis and BLAST program.[33]

Bacterial Strains, Plasmids, Culture techniques, and Media.

Pactamycin producing *S. pactum* ATCC 27456 was purchased from American Type Culture Collection (ATCC). *S. pactum* and its derivatives were grown on BTT agar [glucose (1%), yeast extract (0.1%), beef extract (0.1%), casein hydrolysate (0.2%), agar (1.5%), pH 7.4] at 30 °C for 3 days. Single colonies were used to inoculate the BTT seed cultures and incubated at 30 °C for 3 days. Production cultures were prepared in modified Bennett medium and inoculated with seed cultures [10% (v/v)].[3] The production cultures were incubated at 30 °C for 5 days under vigorous shaking (200 rpm). *Escherichia coli* DH10B was used as a host strain for the construction of recombinant plasmids. *E. coli* ET12567 (pUZ8002) was used as donor strain in conjugation experiments. pBlueScript II (SK-) (Stratagene) and pGEM-T Easy (Promega) were used as cloning vectors. pTMN002, a pJTU1278+ derivative containing apramycin-resistance cassette, was used as vector for gene inactivation.[3,34] *E. coli* BL21(DE3)pLysS and *E. coli* Lemo21(DE3) were used as heterologous hosts for recombinant protein production. All bacterial strains and plasmids used in this study are listed in Supplementary Table 3 and Table 4. Construction, genetic complementation, and analysis of *ptmS*, *ptmI*, *ptmK*::*aac(3)IV*, *ptmO* and *ptmJ* mutants have been described in our previous publications.[3,10]

Construction of *ptmH*/ *ptmI*, *ptmH*/*ptmK*::*aac(3)IV*, and *ptmH*/ *ptmO* mutants.

The target genes were inactivated using gene in-frame deletion strategy (Supplementary Figure 1a). Two ~1 kb PCR fragments upstream (*Hin*dIII/*Eco*RI) and downstream (*Eco*RI/*Xba*I) of the *ptmI* or *ptmO* genes were fused and cloned into the *Hin*dIII/XbaI sites of pBluescript II SK(−) vector. The PCR products of *ptmI* and *ptmO* were excised and cloned into the *Hin*dIII/*Xba*I sites of pTMN002 to generate pTMM052 and pTMM08, respectively. All plasmids were then individually introduced into the *ptmH* mutant strain of *S. pactum* by conjugation using the *E. coli* donor strain ET12567/pUZ8002. Apramycin resistant strains representing single crossover mutants were obtained and subsequently grown on BTT agar plates containing apramycin (50 μg/mL). Apramycin sensitive colonies were counter-selected by replica plating on BTT agar with and without apramycin (50 μg/mL). The resulting double-crossover candidate strains were confirmed by PCR amplification with F1 and R2 primers flanking the respective targeted gene (Supplementary Figure 2).

Construction of *ptmH*/*ptmK*::*aac(3)IV*. The *ptmK* gene (1.7 kb) was inactivated using a gene disruption strategy (Supplementary Figure 1b). The internal fragment (0.88 kb) of *ptmK* was generated by PCR using a forward primer containing a *Hin*dIII site and a reverse primer containing a *Xba*I site (Supplementary Table 5), and *S. pactum* genomic DNA as a template. The PCR product was cloned into the *Hin*dIII/Xbal sites of pTMN002 to generate pTMM055. Plasmid pTMM055 was introduced into the *S. pactum* *ptmH* strain by conjugation, as described by Lu et al.[14] The freshly harvested spores and the overnight-grown *E. coli* ET12567/pUZ8002 containing plasmid pTMM055 were mixed and plated onto MS agar plates containing MgCl$_2$ (10 mM). After incubation at 30 °C for 18 h, the plates were overlaid with sterile water (1 mL) containing nalidixic acid (1 mg/mL) and apramycin (1 mg/mL) and incubated at 30 °C for 5–7 days. The exconjugant (single crossover) colonies were purified by plating onto BTT agar plates supplemented with

apramycin (50 μg/mL). Disruption of *ptmK* was confirmed by PCR amplification
(Supplementary Figure 2).

Analysis of *ptmH/ ptmI*, *ptmH/ ptmO*, and *ptmH/ptmK::aac(3)IV* mutant strains metabolic profiles.

The *ptmH/ ptmI*, *ptmH/ ptmO*, and *ptmH/ptmK::aac(3)IV* strains were grown on BTT
agar at 30 °C for 3 days. Single colonies were used to inoculate the BTT seed cultures
[medium for *ptmH/ptmK::aac(3)IV* was supplemented with apramycin (10 μg/mL) and
ampicillin (20 μg/mL)] and incubated at 30 °C for 2 days. Production cultures were prepared
in modified Bennett's medium (50 mL)[3] and inoculated with seed cultures [10% (V/V)].
The production cultures were incubated at 30 °C for 5 days under vigorous shaking (200
rpm). The mycelia were centrifuged and the supernatants were extracted twice with equal
volumes of EtOAc followed by extraction with *n*-BuOH. The organic solvent from each
extraction was evaporated *in vacuo* and the residues dissolved in MeOH and analyzed by
ESI-MS. The phenotypes/products are listed in Supplementary Table 6.

Chemical complementation of *ptmI*, *ptmH/ ptmI*, *ptmO*, *ptmH/ ptmO*, *ptmS*, *ptmK*, and *ptmK::aprR* mutant strains with 3-[3-aminophenyl]3-oxopropionyl-SNAC.

ptmS,[10] *ptmI*,[10] *ptmK::aprR*,[10] *ptmO*,[10] *ptmH/ ptmI*, *ptmH/ ptmO*, and *ptmH/
ptmK::aprR* mutant strains were streaked on BTT agar [glucose (1%), yeast extract (0.1%),
beef extract (0.1%), casein hydrolysate (0.2%), agar (1.5%), pH 7.4] and incubated at 30 °C
for 3 days. Spores of the mutant strains were grown in Erlenmeyer flasks (125 mL) each
containing 30 mL seed medium [glucose (1%), yeast extract (0.1%), beef extract (0.1%),
casein hydrolysate (0.2%), pH 7.4] for 3 days at 28°C and 200 rpm. The seed cultures of
each strain (1 mL each) were used to inoculate 2×50 mL Erlenmeyer flasks containing
production medium, modified Bennett medium [glucose (1%), yeast extract (0.1%), beef
extract (0.1%), soytone (0.2%), pH 7.4] (10 mL in each flask). After incubation for 16 h
under the same condition, each mutant strain was fed with 3.0 mM of 3AP-3OP-SNAC and
the last flask of each strain was used as a control (no feeding). The feeding was repeated
every 12 h for 2 days. After 5 days of incubation, the cultures were centrifuged and the
metabolites of each group were extracted twice with equal volume of EtOAc and once with
1.5 volume of *n*-BuOH. The organic solvent was evaporated *in vacuo*. The residues were
dissolved in MeOH and were analyzed by MS and HPLC. The phenotypes/products are
listed in Supplementary Table 6.

Other incorporation studies with 3ABA-SNAC, GlcNAc-3ABA, [^{13}C]GlcNAc-[^{13}C]3ABA,
aniline, 3-fluoroaniline, 4-fluoroaniline, and 3AAP to various mutants of *S. pactum* were
carried out using a similar procedure as described above.

Cloning and expression of *ptmS*.

The *ptmS* gene was amplified using the primers *ptmS-Eco*RI and *ptmS-Hin*dIII
(Supplementary Table 5). The PCR product was cloned into the *Eco*RI and *Hin*dIII sites of
pMBP-28 B to generate the expression vector pMBP-28 B-*ptmS*, which was then transferred
into *E. coli* BL21(DE3)pLysS (Invitrogen). The empty vector pMBP-28 B was introduced
into *E. coli* BL21(DE3)pLysS to be used as a control. For expression of MBP-PtmS fusion

protein, the bacteria were grown in LB medium supplemented with kanamycin (50 μg/mL) and chloramphenicol (50 μg/mL) at 37 °C for 16 h. An aliquot (2 mL) of overnight grown culture was used to inoculate a fresh LB medium (200 mL in 1000 mL flask), supplemented with the same antibiotics, at 37 °C with shaking (200 rpm) until OD_{600} reached 0.5. Recombinant protein expression was induced with isopropyl β-D-thiogalactopyranoside (IPTG) to a final concentration of 0.3 mM and the culture was further cultivated for 8 h. The cells were harvested by centrifugation (4200 rpm, 10 min, 4 °C) and stored at −80 °C until used.

Cloning and expression of *ptmI, ptmP, and sfp*.

The *ptmI* gene was amplified using the primers *ptmI-EcoRI* and *ptmI-Hin*dIII (Supplementary Table 5). The PCR product was cloned into the *Eco*RI and *Hin*dIII sites of pACYCDuet-1 to generate the expression vector pACYCDuet-1-*ptmI*. *For* co-expression of *PtmI* and *PtmP* (to obtain holo-PtmI), the *ptmP* gene was amplified using the primers *ptmP-Nde*I and *ptmP-Xho*I and the PCR product was cloned into the *Nde*I and *Xho*I sites of the pACYCDuet-1-*ptmI* construct to produce the expression vector pACYCDuet-1-*ptmI-ptmP*. On the other hand, *sfp* gene was amplified using the primers *sfp-Nde*I and *sfp-Xho*I and the plasmid pUC8-*sfp* was used as a template. The PCR product was cloned into the *Nde*I and *Xho*I sites of pET28a to generate the expression vector pET28a-*sfp*. Each expression plasmid was transferred into *E. coli* BL21(DE3). In addition, to obtain holo-PtmI, both pACYCDuet-1-*ptmI* and pET28a-*sfp* were transferred into *E. coli* BL21(DE3). For the expression of apo-PtmI, the *E. coli* BL21(DE3) harboring pACYCDuet-1-*ptmI* construct was grown in LB medium supplemented with chloramphenicol (50 μg/mL) at 37 °C for 16 h. An aliquot (2 mL) of overnight grown culture were used to inoculate a fresh LB medium (200 mL in 1000 mL flask), supplemented with the same antibiotic, and was grown at 37 °C with shaking (200 rpm) until an OD_{600} of 0.5 was reached. Then, the temperature was reduced to 30°C and IPTG was added to a final concentration of 0.3 mM to induce protein expression. After further growth for 8 h, the cells were harvested by centrifugation (4200 rpm, 10 min, 4 °C) and stored at −80 °C until used. The PtmI was co-expressed with PtmP and Sfp individually using the same protocol of Apo-PtmI expression described above.

Cloning and expression of *ptmK*.

The *ptmK* gene was amplified using the primers *ptmK-Eco*RI and *ptmK-Hin*dIII (Supplementary Table 5). The PCR product was cloned into the *Eco*RI and *Hin*dIII sites of pET28a to generate the expression vector pET28a-*ptmK*. The pET28a-*ptmK* construct was transferred into *E. coli* Lemo21 (Invitrogen). The empty vector pET28a was also transferred into *E. coli* Lemo21 to be used as a control. To express *ptmK*, the *E. coli* Lemo21 harboring pET28a-*ptmK* was cultivated in LB medium supplemented with kanamycin (50 μg/mL) and chloramphenicol (50 μg/mL) at 37 °C for 16 h. Subsequently, the overnight grown culture (2 mL) was transferred to a fresh LB medium (200 mL in 1000 mL flask), supplemented with kanamycin (50 μg/mL), chloramphenicol (50 μg/mL), and L-rhamnose (80 μM) and grown at 37 °C until OD_{600} reached 0.5. Then, the temperature was reduced to 30 °C and IPTG was added to a final concentration of 0.4 mM to induce protein expression. After further growth for 10 h, the cells were harvested by centrifugation (4200 rpm, 10 min, 4 °C) and stored at −80 °C until used.

Cloning and expression of *ptmO*.

The *ptmO* gene was amplified using the primers *ptmO-Bgl*II and *ptmO-Eco*RI (Supplementary Table 5). The PCR product was cloned into the *Bam*HI and *Eco*RI sites of the pRSET B to generate the expression vector pTMM080 (pRSET B-*ptmO*), which was then introduced into *E. coli* BL21(DE3)pLysS (Invitrogen). The empty vector pRSET B was also introduced into *E. coli* BL21(DE3)pLysS and used as a control. For the expression of *ptmO*, the bacteria were grown in LB medium supplemented with chloramphenicol (50 μg/mL) and ampicillin (100 μg/mL) at 37 °C for 16 h. An aliquot (2 mL) of the overnight grown culture was used to inoculate a fresh LB medium (200 mL in 1000 mL flask), supplemented with the same antibiotics, at 37 °C with shaking (200 rpm) and was grown until an OD600 of 0.5 was reached. Then, the temperature was reduced to 30 °C and isopropyl β-D-thiogalactopyranoside (IPTG) was added to a final concentration of 0.3 mM to induce protein expression. After further growth for 8 h, the cells were harvested by centrifugation (4200 rpm, 10 min, 4 °C) and stored at −80 °C until used.

Cloning and expression of *ptmJ*.

The *ptmJ* gene was amplified using the primers *ptmJ-Nde*I and *ptmJ-Eco*RI. The PCR product was cloned into the *Nde*I and *Eco*RI sites of pET-28a and was subsequently transferred into *E. coli* Lemo21(DE3). For the expression of *ptmJ*, the bacteria were grown in LB medium supplemented with chloramphenicol (50 μg/mL) and kanamycin (50 μg/mL) at 37 °C for 16 h. An aliquot (2 mL) of the overnight grown culture was used to inoculate a fresh LB medium (200 mL in 1000 mL flask), supplemented with kanamycin (50 μg/mL), chloramphenicol (50 μg/mL), and L-rhamnose (80 μM) and grown at 37 °C with shaking (200 rpm) until an OD600 of 0.5 was reached. Then, the temperature was reduced to 30 °C and IPTG was added to a final concentration of 0.4 mM to induce protein expression. After further growth for 10 h, the cells were harvested by centrifugation (4200 rpm, 10 min, 4 °C) and stored at −80 °C until used.

Enzyme assay of PtmS.

PtmS assay was done in a reaction (100 μL) containing Tris-HCl (50 mM, pH 8.0), ATP (5 mM), $MgCl_2$ (5 mM), DTT (1 mM), 3ABA (2 mM) and PtmS (10 μM). The reaction was performed at 30 °C for 5 h. The reaction was then quenched with an equal volume of MeOH, centrifuged, and the supernatant (20 μL) was analyzed by LC-MS [Zorbax SB-C18 column, 4.6×150 mm, 5 μm; solvent A: H_2O (contains 0.1% TFA), solvent B: CH_3CN (contains 0.1% TFA), gradient 2% – 100% solvent B over 55 min; flow-rate 0.5 mL/min].

The measurement of inorganic pyrophosphate (PP_i) production was performed using a coupled colorimetric assay using pyrophosphatase and purine nucleoside phosphorylase. The PtmS enzymatic reaction solutions (5 μL or 10 μL) were added to the enzyme solution containing pyrophosphatase (5 μL) and purine nucleoside phosphorylase (10 μL), MESG (200 μL), 50x buffer (50 μL) and ddH_2O (up to 1000 μL). The mixture was then incubated for 1 h at 22 °C. The change in absorbance at 360 nm was obtained in triplicate from distinct samples after subtracting the background absorbance.

Formation of 3-aminobenzoyl-PtmI.

PtmS assay was done in a reaction (100 μL) containing Tris-HCl (50 mM, pH 8.0), ATP (5 mM), MgCl$_2$ (5 mM), DTT (1 mM), 3ABA (2 mM), holo-PtmI/Sfp (200 μM), and PtmS (10 μM). The reaction was performed at 30 °C for 5 h. The reaction mixture was partially desalted with Tris-HCl buffer (20 mM, pH 8.0) using a 3 KDa MWCO size-exclusion filter, the solution was then analyzed by LC-MS [Mab Pac RP LC analytical column, 1 × 150 mm, 4 μm; solvent A: H$_2$O, solvent B: CH$_3$CN, gradient 0% – 100% solvent B over 20 min; flow-rate 0.1 mL/min]. Boiled PtmS was used as a negative control.

The measurement of AMP production was performed using the AMP-Glo™ assay (Promega). The PtmS/PtmI enzymatic reaction solutions (10 μL) were diluted with Tris-HCl buffer (15 μL), mixed with the AMP-Glo™ Reagent I (25 μL), and incubated for 60 min to terminate the reaction, remove any remaining ATP, and convert AMP to ADP. Subsequently, AMP detection solution (a mixture of AMP-Glo™ Reagent II and Kinase-Glo One Solution) (50 μL) was added to the mixture and incubated for 60 min to drive the conversion of ADP to ATP. The ATP was detected through the luciferase reaction. The change in luminescence was obtained in triplicate from distinct samples after subtracting the background emission using BioTek Synergy HT microplate reader with the Gen5 2.07 software.

Malonylation of the acyl carrier protein PtmI.

Malonylation of PtmI was achieved by incubation of PtmI (200 μM in 50 mM Tris HCl, 500 mM NaCl, pH 8.0) with malonyl-CoA (8 mM) for 7 h at 30°C. The reaction was processed and analyzed by LC-MS as described for 3-aminobenzoyl-PtmI above.

Enzyme assay of PtmK (formation of β-ketoacyl-PtmI).

PtmK (20 μM) was preacylated by incubation with 3ABA-PtmI at 30 °C for 12 h. Then the acyl-PtmK was mixed with malonyl-PtmI in a 1:1 ratio. The reaction was allowed to proceed for 16 h and the product was analyzed by LC-MS as described above.

Enzyme assay of PtmO.

After formation of β-ketoacyl-PtmI, the hydrolase enzyme PtmO was added to the reaction mixture and incubation was extended at 30 °C for 7 h. The reaction was quenched by adding an equal volume of MeOH, centrifuged, and the product was analyzed by HPLC.

Enzyme assay of PtmJ.

After the formation of 3ABA-PtmI or β-ketoacyl-PtmI, the glycosyltransferase enzyme PtmJ (10 μM), UDP-GlcNAc (5 mM), and MgCl$_2$ (2 mM) were added and the reaction mixtures were incubated at 30 °C for 10 h. The products were analyzed by LC-MS as described above.

The UDP production was determined by using the phosphopyruvate kinase (PK) and lactate dehydrogenase (LDH) coupled assay (Sigma-Aldrich). The reaction mixture (200 μL) contained PtmJ reaction mixture (150 μL), phosphoenolpyruvate (1.6 mM), NADH (0.1 mM), PK (37 U), and LDH (55.8 U). Oxidation of NADH to NAD$^+$ was monitored in a 96-well plate using a spectrophotometric microplate reader at 340 nm. Reaction mixtures with

boiled PtmJ were used as negative control (blank). The data were collected in triplicate from distinct samples.

Data Availability

All data that support the conclusions are available from the authors on request.

Supplementary Material

Refer to Web version on PubMed Central for supplementary material.

Acknowledgements

REFERENCES

1. Mao Y, Varoglu M & Sherman DH Molecular characterization and analysis of the biosynthetic gene cluster for the antitumor antibiotic mitomycin C from *Streptomyces lavendulae* NRRL 2564. Chem Biol 6, 251–263 (1999). [PubMed: 10099135]

2. Kudo F, Kasama Y, Hirayama T & Eguchi T Cloning of the pactamycin biosynthetic gene cluster and characterization of a crucial glycosyltransferase prior to a unique cyclopentane ring formation. J Antibiot 60, 492–503 (2007). [PubMed: 17827660]

3. Ito T et al. Deciphering pactamycin biosynthesis and engineered production of new pactamycin analogues. ChemBioChem 10, 2253–2265 (2009). [PubMed: 19670201]

4. Rinehart KL Jr., Weller DD & Pearce CJ Recent biosynthetic studies on antibiotics. J. Nat. Prod 43, 1–20 (1980).

5. Almabruk KH et al. Mutasynthesis of fluorinated pactamycin analogues and their antimalarial activity. Org Lett 15, 1678–1681 (2013). [PubMed: 23521145]

6. Hirayama A, Eguchi T & Kudo F A Single PLP-Dependent Enzyme PctV Catalyzes the Transformation of 3-Dehydroshikimate into 3-Aminobenzoate in the Biosynthesis of Pactamycin. ChemBioChem 14, 1198–1203 (2013). [PubMed: 23744829]

7. Rinehart KL Jr. Biosynthesis and mutasynthesis of aminocyclitol antibiotics. Jpn J Antibiot 32 Suppl, S32–46 (1979). [PubMed: 398906]

8. Hirayama A, Miyanaga A, Kudo F & Eguchi T Mechanism-Based Trapping of the Quinonoid Intermediate by Using the K276R Mutant of PLP-Dependent 3-Aminobenzoate Synthase PctV in the Biosynthesis of Pactamycin. ChemBioChem 16, 2484–2490 (2015). [PubMed: 26426567]

9. Abugrain ME et al. Interrogating the Tailoring Steps of Pactamycin Biosynthesis and Accessing New Pactamycin Analogues. ChemBioChem 17, 1585–1588 (2016). [PubMed: 27305101]

10. Abugrain ME, Brumsted CJ, Osborn AR, Philmus B & Mahmud T A Highly Promiscuous β-Ketoacyl-ACP Synthase (KAS) III-like Protein Is Involved in Pactamycin Biosynthesis. ACS Chem Biol 12, 362–366 (2017). [PubMed: 28060484]

11. Bibb MJ, Sherman DH, Omura S & Hopwood DA Cloning, sequencing and deduced functions of a cluster of *Streptomyces* genes probably encoding biosynthesis of the polyketide antibiotic frenolicin. Gene 142, 31–39 (1994). [PubMed: 8181754]

12. Ahlert J et al. The calicheamicin gene cluster and its iterative type I enediyne PKS. Science 297, 1173–1176 (2002). [PubMed: 12183629]

13. Mao Y, Varoglu M & Sherman DH Genetic localization and molecular characterization of two key genes (mitAB) required for biosynthesis of the antitumor antibiotic mitomycin C. J Bacteriol 181, 2199–2208 (1999). [PubMed: 10094699]

14. Lu W, Roongsawang N & Mahmud T Biosynthetic studies and genetic engineering of pactamycin analogs with improved selectivity toward malarial parasites. Chem Biol 18, 425–431 (2011). [PubMed: 21513878]

15. Upson RH, Haugland RP, Malekzadeh MN & Haugland RP A spectrophotometric method to measure enzymatic activity in reactions that generate inorganic pyrophosphate. Anal Biochem 243, 41–45 (1996). [PubMed: 8954523]

16. Yang J et al. Nucleotidylation of unsaturated carbasugar in validamycin biosynthesis. Org Biomol Chem 9, 438–449 (2011). [PubMed: 20981366]

17. Jia XY et al. Genetic characterization of the chlorothricin gene cluster as a model for spirotetronate antibiotic biosynthesis. Chem Biol 13, 575–585 (2006). [PubMed: 16793515]

18. Mondal S, Hsiao K & Goueli SA Utility of Adenosine Monophosphate Detection System for Monitoring the Activities of Diverse Enzyme Reactions. Assay Drug Dev Technol 15, 330–341 (2017). [PubMed: 29120675]

19. Asamizu S, Yang J, Almabruk KH & Mahmud T Pseudoglycosyltransferase catalyzes nonglycosidic C-N coupling in validamycin a biosynthesis. J Am Chem Soc 133, 12124–12135 (2011). [PubMed: 21766819]

20. Adams ES & Rinehart KL Directed biosynthesis of 5''-fluoropactamycin in *Streptomyces pactum*. J Antibiot 47, 1456–1465 (1994). [PubMed: 7844040]

21. Schmelz S & Naismith JH Adenylate-forming enzymes. Curr Opin Struct Biol 19, 666–671 (2009). [PubMed: 19836944]

22. August PR et al. Biosynthesis of the ansamycin antibiotic rifamycin: deductions from the molecular analysis of the rif biosynthetic gene cluster of *Amycolatopsis mediterranei* S699. Chem Biol 5, 69–79 (1998). [PubMed: 9512878]

23. Yu TW et al. The biosynthetic gene cluster of the maytansinoid antitumor agent ansamitocin from *Actinosynnema pretiosum*. Proc Natl Acad Sci U S A 99, 7968–7973 (2002). [PubMed: 12060743]

24. Admiraal SJ, Khosla C & Walsh CT A Switch for the transfer of substrate between nonribosomal peptide and polyketide modules of the rifamycin synthetase assembly line. J Am Chem Soc 125, 13664–13665 (2003). [PubMed: 14599196]

25. Zawada RJ & Khosla C Domain analysis of the molecular recognition features of aromatic polyketide synthase subunits. J Biol Chem 272, 16184–16188 (1997). [PubMed: 9195917]

26. Sherman DH, Kim ES, Bibb MJ & Hopwood DA Functional replacement of genes for individual polyketide synthase components in *Streptomyces coelicolor* A3(2) by heterologous genes from a different polyketide pathway. J Bacteriol 174, 6184–6190 (1992). [PubMed: 1400167]

27. Lu W, Alanzi AR, Abugrain ME, Ito T & Mahmud T Global and pathway-specific transcriptional regulations of pactamycin biosynthesis in *Streptomyces pactum*. Appl Microbiol Biotechnol 102, 10589–10601 (2018). [PubMed: 30276712]

28. Hirayama A, Chu J, Goto E, Kudo F & Eguchi T NAD^+-Dependent Dehydrogenase PctP and Pyridoxal 5'-Phosphate Dependent Aminotransferase PctC Catalyze the First Postglycosylation Modification of the Sugar Intermediate in Pactamycin Biosynthesis. ChemBioChem 19, 126–130 (2018). [PubMed: 29148266]

29. Lombard V, Golaconda Ramulu H, Drula E, Coutinho PM & Henrissat B The carbohydrate-active enzymes database (CAZy) in 2013. Nucleic Acids Res 42, D490–495 (2014). [PubMed: 24270786]

30. Kieser T, Bibb MJ, Buttner MJ, Chater KF & Hopwood DA Practical Streptomyces Genetics (The John Innes Foundation, Norwich, 2000).

31. Green MR & Sambrook J Molecular Cloning. A Laboratory Manual (Cold Spring Harbor Laboratory Press, Cold Spring Harbor, New York, 2012).

32. Ishikawa J & Hotta K FramePlot: a new implementation of the frame analysis for predicting protein-coding regions in bacterial DNA with a high G + C content. FEMS Microbiol Lett 174, 251–253 (1999). [PubMed: 10339816]

33. Altschul SF, Gish W, Miller W, Myers EW & Lipman DJ Basic local alignment search tool. J Mol Biol 215, 403–410 (1990). [PubMed: 2231712]

34. He Y et al. Two pHZ1358-derivative vectors for efficient gene knockout in *Streptomyces*. J Microbiol Biotechnol 20, 678–682 (2010). [PubMed: 20467238]

Figure 1. Proposed biosynthetic pathways to pactamycin.
a. Biosynthetic origin of pactamycin structural components; **b**. Previously proposed pathways to pactamycin; **c.** Biosynthetic gene cluster of pactamycin in *Streptomyces pactum*. Colored thick arrows represent genes that are directly involved in this study.
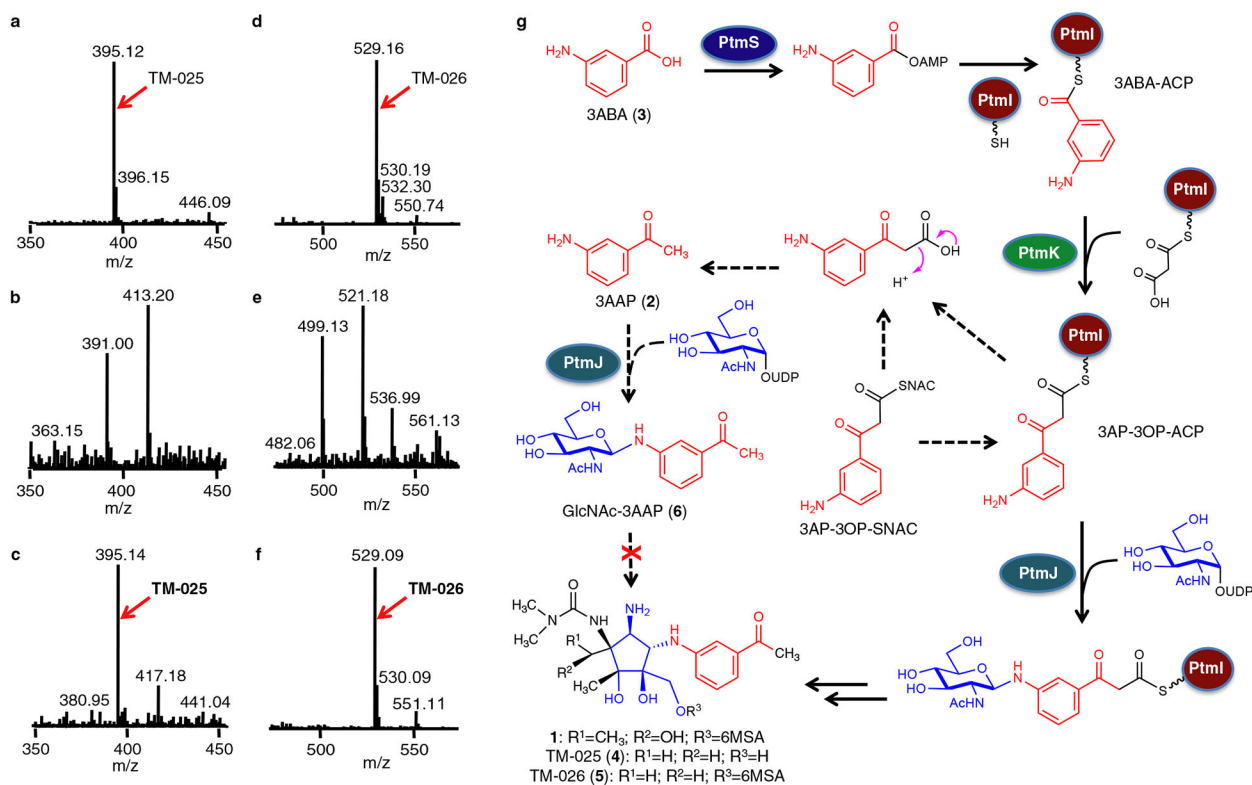
Figure 2.

In vivo evidence for the involvement of 3AP-3OP-ACP in pactamycin biosynthesis. Representative mass spectrum of **a**. the BuOH extract of Δ*ptmH* showing the presence of TM-025; **b**. the BuOH extract of Δ*ptmH*/Δ*ptmT* showing the absent of TM-025; **c**. the BuOH extract of Δ*ptmH*/Δ*ptmT* complemented with 3AP-3OP-SNAC showing the recovery of TM-025 production; **d**. the EtOAc extract of Δ*ptmH* showing the presence of TM-026; **e**. the EtOAc extract of Δ*ptmH*/Δ*ptmT* showing the absent of TM-026; **f**. the EtOAc extract of Δ*ptmH*/Δ*ptmT* complemented with 3AP-3OP-SNAC showing the recovery of TM-026 production; **g**. A newly proposed biosynthetic pathway to pactamycin showing that glycosylation occurs on an ACP-bound polyketide intermediate. Experiments 2a-f were performed independently three times with similar results.
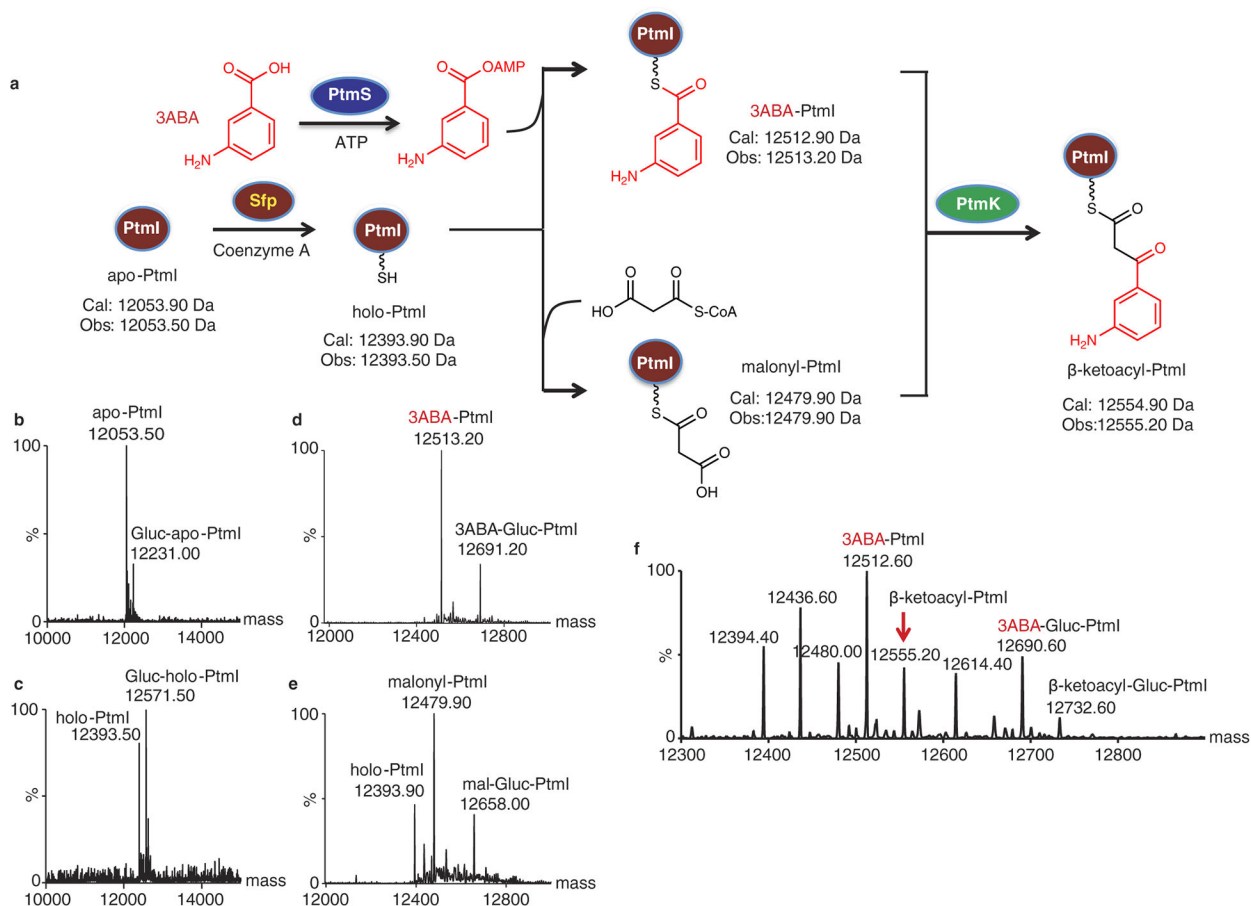
Figure 3.
Loading of 3ABA to the acyl-carrier protein PtmI and formation of β-ketoacyl-PtmI. **a**. Conversion of apo-PtmI to holo-PtmI, loading of 3ABA or malonate to PtmI, and decarboxylative Claisen condensation of 3ABA-PtmI and malonyl-PtmI to give β-ketoacyl-PtmI; **b.** Deconvoluted mass spectrum of apo-PtmI; **c**. Deconvoluted mass spectrum of holo-PtmI; **d**. Deconvoluted mass spectrum of a reaction mixture containing holo-PtmI, PtmS, 3ABA, ATP and $MgCl_2$; **e.** Deconvoluted mass spectrum of holo-PtmI incubation with malonyl-CoA; **f.** Deconvoluted mass spectrum of PtmK incubation with 3ABA-PtmI and malonyl-PtmI. The gluconoylated proteins are labeled with "Gluc". Decarboxylation of malonyl-PtmI (12480.00 Da) and its Gluc analogue (12658.40 Da) yielded acetyl-PtmI (12436.60 Da) and its Gluc analogue (12614.40 Da), respectively. Experiments 3b-f were performed independently three times with similar results.
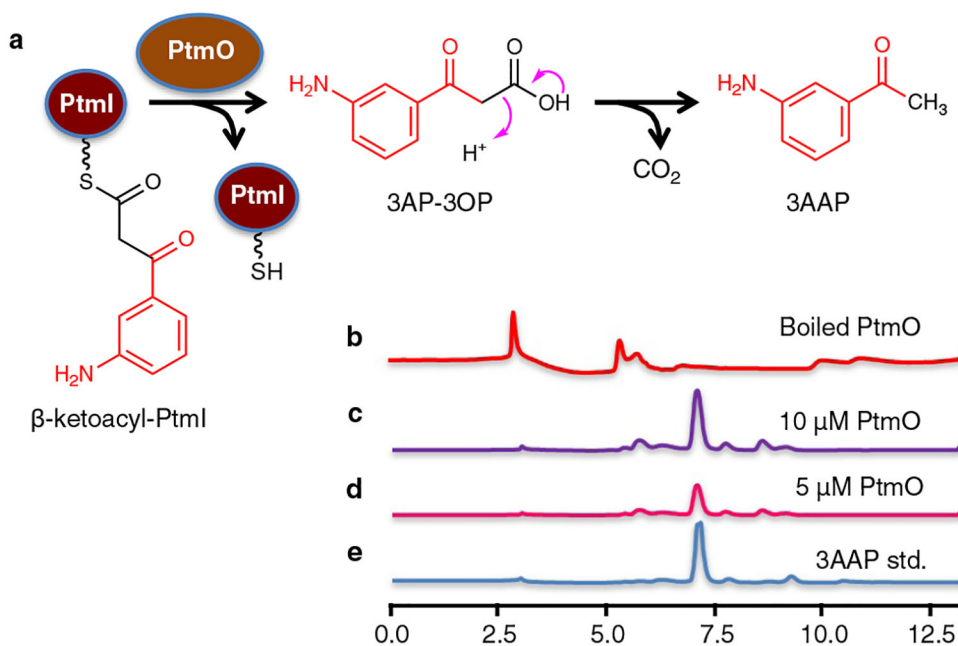
Figure 4.
Biochemical characterization of PtmO. **a**. Incubation of 3AP-3OP-PtmI with recombinant PtmO resulted in 3AAP; **b**. HPLC chromatogram of enzymatic reaction with boiled PtmO; **c**. HPLC chromatogram of enzymatic reaction with 10 μM PtmO; **d**. HPLC chromatogram of enzymatic reaction with 5 μM PtmO; **e**. HPLC chromatogram of standard 3-aminoacetophenone (3AAP). HPLC chromatograms were recorded based on UV absorption at 254 nm. Experiments 4b-d were performed independently at least three times with similar results.

Figure 5.
In vitro reconstitution of the PKS and the glycosyltransferase proteins involved in pactamycin biosynthesis. **a**. Enzymatic reactions from 3ABA to GlcNac-3ABA-PtmI and to GlcNAc-β-ketoacyl-PtmI; **b**. Deconvoluted mass spectrum of a reaction mixture containing PtmS, PtmI, and PtmJ; **c**. Deconvoluted mass spectrum of a reaction mixture with PtmS, PtmI, PtmK, and PtmJ; **d**. Deconvoluted mass spectrum of a reaction mixture with PtmS, PtmI, PtmK, and PtmJ using 3ABA-2,4,5,6-d_4 as substrate; **e**. Deconvoluted mass spectrum of a reaction mixture with PtmS, PtmI, PtmK, and boiled PtmJ. Magenta circle, holo-PtmI; blue circle, acetyl-PtmI; black circle, malonyl-PtmI; red diamond, 3ABA-PtmI; purple triangle, 3AP-3OP-PtmI; orange star, GlcNAc-3ABA-PtmI; yellow star, GlcNAc-3AP-3OP-PtmI. The gluconoylated proteins are labeled with "Gluc". Deuterated species are labeled with d_4. Experiments 5b-e were performed independently at least three times with similar results.

Figure 6.
Characterization of the substrate selectivity of PtmK. **a**. experimental design for PtmK selectivity using 3ABA-SNAC as substrate; **b**. mass spectrum of PtmJ reaction mixture showing that 3ABA-SNAC can be glycosylated to give GlcNAc-3ABA-SNAC; **c**. deconvoluted mass spectrum of PtmK reaction mixture showing that only β-ketoacyl-PtmI was produced. Experiments 6b-c were performed independently three times with similar results.